

TrueCISS: Genuine bSSFP Signal Reconstruction from Undersampled Multiple-Acquisition SSFP Using Model-Based Iterative Non-Linear Inversion

Tom Hilbert^{1,2}, Damien Nguyen³, Tobias Kober^{1,2}, Jean-Philippe Thiran², Gunnar Krueger^{1,2}, and Oliver Bieri³

¹Siemens ACIT – CHUV Radiology, Siemens Healthcare IM BM PI & Department of Radiology CHUV, Lausanne, Switzerland, ²LTS5, École Polytechnique Fédérale de Lausanne, Lausanne, Switzerland, ³Radiological Physics, Department of Radiology, University of Basel, Basel, Switzerland

PURPOSE: Off-resonances lead to a pronounced and periodic signal modulation of balanced steady-state free precession (bSSFP)¹, commonly perceived in the image as signal voids or banding artifacts that appear at multiples of $\pm 180^\circ$ phase advance within any TR. Constructive Interference in Steady State (CISS) addresses this unavoidable problem by sequentially acquiring two (or more) bSSFP datasets with different radio-frequency (RF) phase cycling schemes that can be combined by different methods, such as sum-of-squares (SOS) or maximum intensity (MI) reconstruction, to yield banding-free images². However, residual signal modulations persist, especially in the low flip angle regime and the reconstructed signal does no longer reflect the genuine bSSFP steady state amplitude. Here, we suggest a new method to acquire and reconstruct the genuine bSSFP signal from undersampled multiple-acquisition SSFP in combination with a model-based iterative non-linear inversion, termed trueCISS.

METHODS: A spherical phantom doped with 0.125mM MnCl₂ (T₁/T₂ ~ 870 / 70 ms) and, after obtaining written consent, one healthy volunteer were scanned at 3T (MAGNETOM Prisma, Siemens Healthcare, Erlangen, Germany) using a 3D bSSFP prototype sequence (resolution 1.3 mm³, TR 3.92 ms, TE 1.96 ms, flip-angle 15°). Eight bSSFP k-spaces were sequentially acquired with different RF phase increments ($\phi = 0^\circ, 45^\circ, 90^\circ, 135^\circ, 180^\circ, 225^\circ, 270^\circ, 315^\circ$). The fully-sampled datasets were artificially fourfold undersampled using the sampling pattern illustrated in Fig. 1. Subsequently, the bSSFP signal-model³ (cf. Eq. 1 with M_0 spin density, Λ relaxation time ratio T₁/T₂, α flip-angle, $\Delta\phi$ local phase offset relating to field inhomogeneity) was fitted onto the undersampled data using a model-based iterative non-linear inversion algorithm⁴, effectively estimating three parameter maps: M_0 , Λ , and $\Delta\phi$. Spatial regularization (total generalized variation⁵) was applied during this optimization procedure. The resulting parameter maps were then used to synthesize an on-resonant bSSFP signal image by applying the forward signal model with $\phi - \Delta\phi = 0^\circ$. The resulting trueCISS images were compared to the contemporary CISS approach (calculated from two fully-sampled bSSFP datasets with $\phi = 0^\circ, 180^\circ$ using SOS image reconstruction).

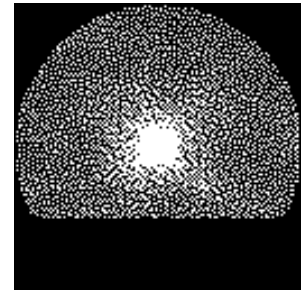


Fig. 1 Sampling pattern of the sequence. White pixels indicate sampled k-space points.

$$\text{Eq. 1} \quad M = M_0 \frac{2 \sin \alpha \cos(\frac{\phi - \Delta\phi}{2})}{1 + \cos \alpha + 2 \cos(\phi - \Delta\phi) + (4\Lambda - \cos(\phi - \Delta\phi)^2) \sin(\frac{\alpha}{2})^2} e^{i(\frac{\phi - \pi}{2})}$$

RESULTS & DISCUSSION: A comparison of the phantom reconstructions using CISS and trueCISS is shown in Fig. 2. Residual banding-related signal modulations persist for the common CISS reconstruction due to the low flip angle used (15° as compared to the optimal one of about 35° for the phantom specific $\Lambda^{-1} \sim 0.1$). In contrast, trueCISS is essentially artifact-free. Moreover, it is directly evident that the CISS signal does not reflect the genuine bSSFP steady state amplitude; even for regions where no banding appears. Similar results are observed for the in-vivo dataset as illustrated in Fig. 3. In the CISS image, a residual signal drop is clearly visible around the nasal cavity caused by incomplete removal of banding artifacts in the low flip angle regime. In comparison, this cannot be observed in the trueCISS image, though minor blurring, induced by spatial regularization, is visible. Generally, a banding-free reconstruction of the genuine bSSFP signal, as with trueCISS, is of high interest for quantitative SSFP imaging (e.g. T₁ or T₂ relaxometry⁶) since any deviation from the bSSFP signal model inevitably yields flawed estimates.

It should be noted that trueCISS does not require additional measurement time compared to a standard CISS acquisition as undersampling compensates for the increase in number of repetitions.

CONCLUSION: TrueCISS imaging is able to provide artifact-free bSSFP images with similar overall acquisition times as CISS. Quantitative imaging methods will particularly benefit from the genuine synthesized bSSFP signal, as provided by trueCISS, although the employed spatial regularization induces blurring in the final image.

REFERENCES: 1. Carr HY. Phys Rev. 1958; 112:1693-1701.

2. Casselman et al, Am J Neuroradiol. 1993; 14:47-57.

3. Bieri O. Magn Reson Med. 2011;65(2):422-31

4. Sumpf, Tilman J et al J Magn Reson Imaging. 2011;34(2) :420-8.

5. Knoll, Florian et al Magn Reson Med. 2011;65(2): 480-91.

6. Deoni SC et al Magn Reson Med. 2004;52(2):435-9.

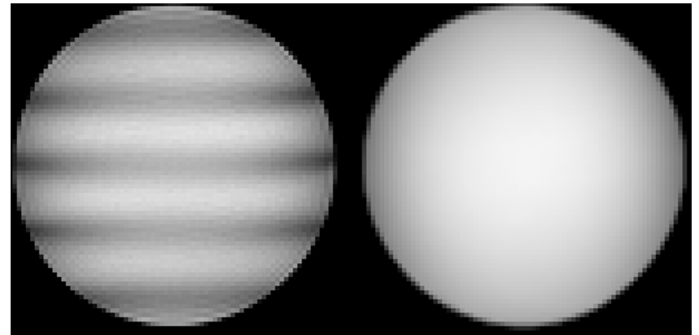


Fig. 2 Reconstructed phantom images using CISS (left) and trueCISS (right) in the presence of a linear frequency offset (from bottom to top).

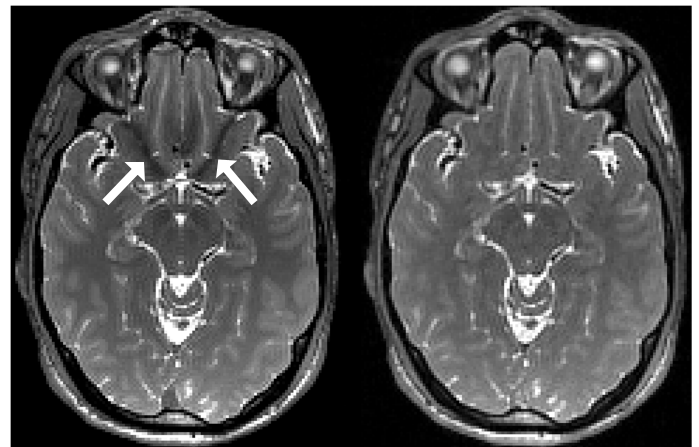


Fig. 3 Reconstructed in-vivo data using CISS (left) and trueCISS (right). The white arrows indicate residual banding-related artifacts.